Expanded View Figures

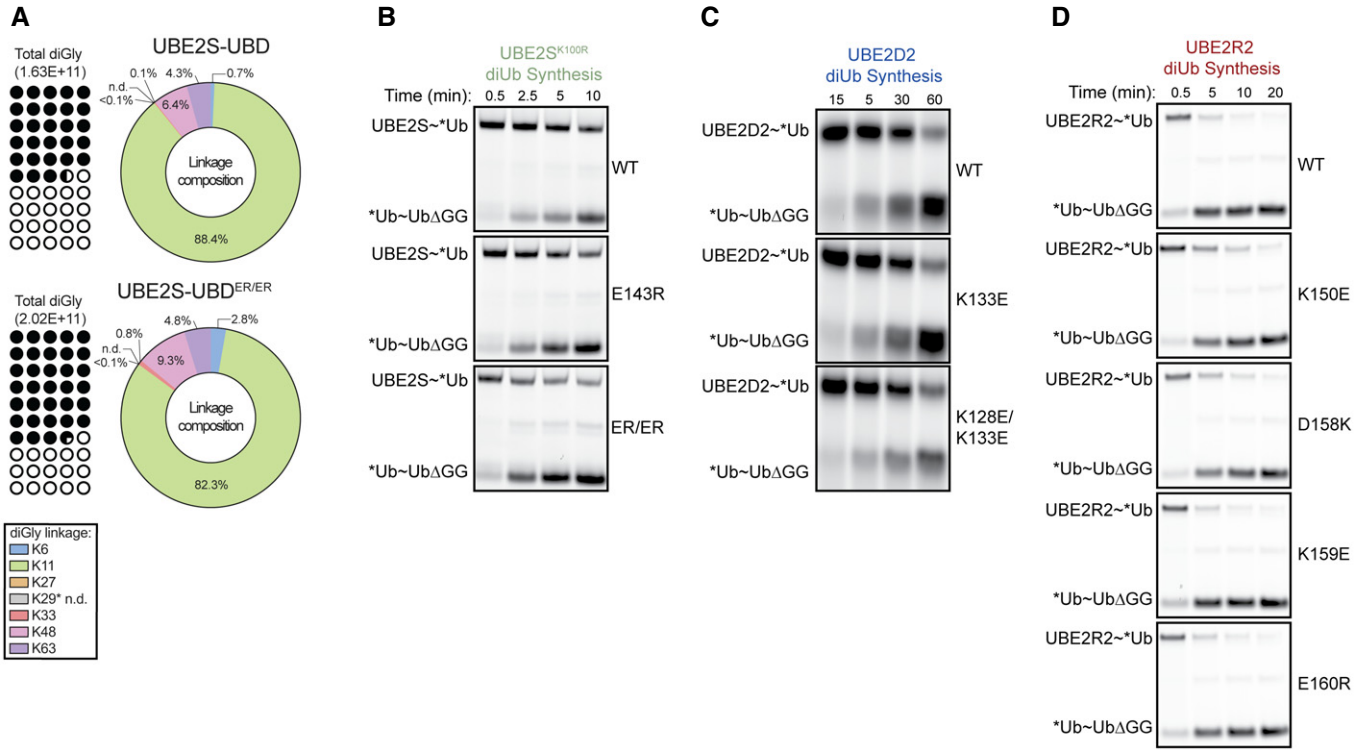

Figure EV1. Charge-swaps at the E2^{HTH} impact activity across several E2 family members.

A A Mass spectrometry analysis of Ub linkages from chain elongation reactions performed by UBE2S-UBD WT and ER/ER (related to Fig 1D and E, and Appendix Fig S1G).

B–D Fluorescent scans monitoring the diUb production by UBE2S (B), UBE2D2 (C), and UBE2R2 (D) WT and charge-swapped variants. The UBE2S, UBE2D2, and UBE2R2 WT panels used in Fig 2E,G,H are shown for comparison.

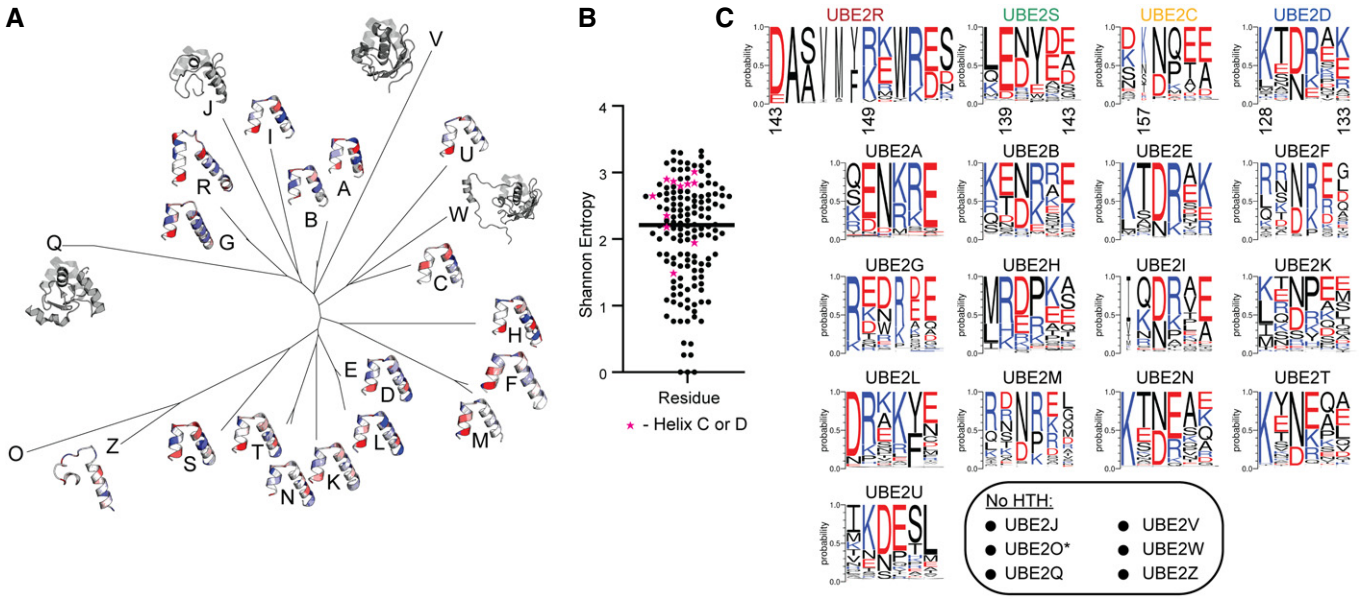

Figure EV2. The HTH is a variable region across E2 family members but retains some charge conservation for individual E2s.

A Maximum likelihood phylogenetic tree of the E2 family, including charge conservation models at the $E2^{HTH}$.

B Shannon entropy plot of residue conservation across the E2 family. The majority of residues in the $E2^{HTH}$ (pink stars) have increased Shannon entropy compared to the E2 mean represented by the horizontal line.

C Weblogos of $E2^{HTH}$ residue conservation for each E2 family member. UBE2S, UBE2C, UBE2D, and UBE2R are repeated from Fig 2I for comparison.

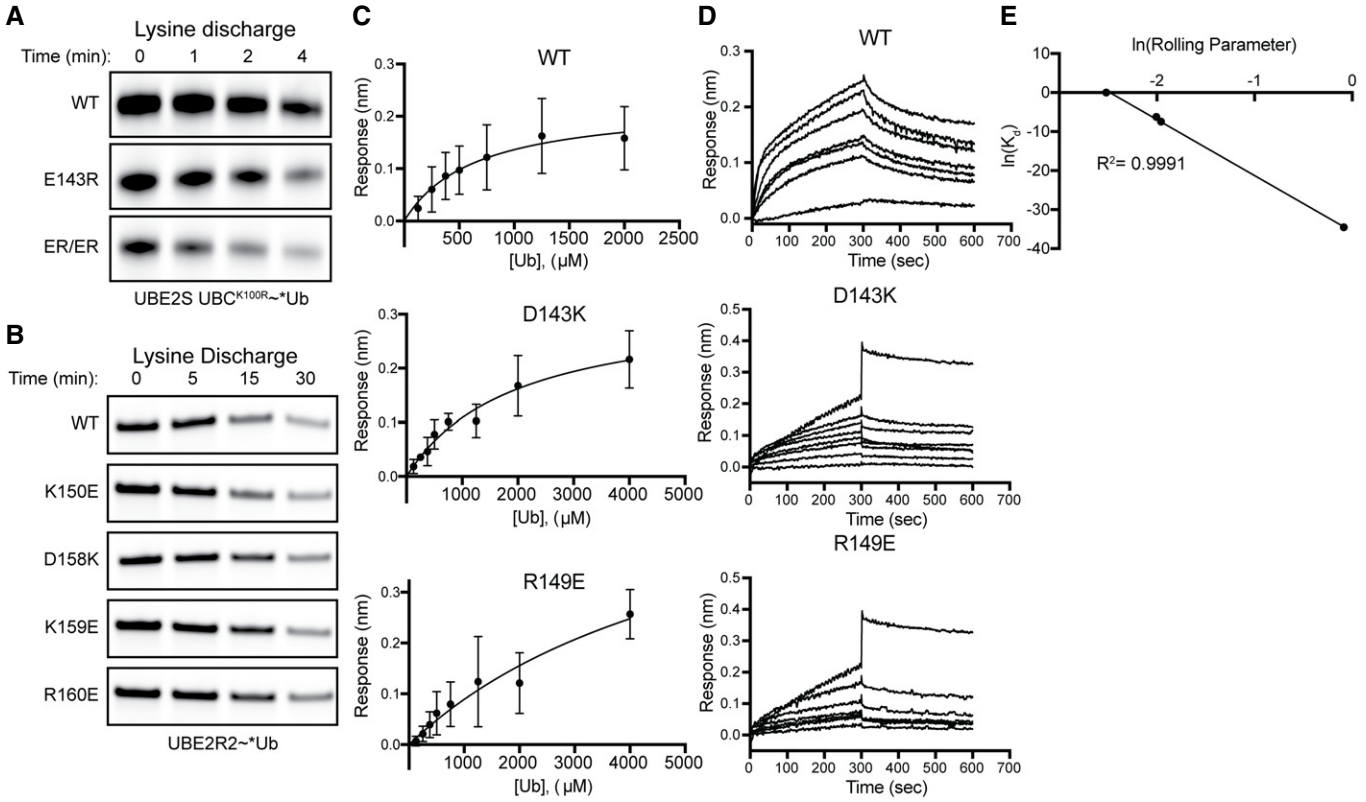

Figure EV3. UBE2R2^{HTH} facilitates acceptor Ub binding for diUb synthesis.

A Fluorescent scan of the lysine discharge assay monitoring the stability of the UBE2S~*Ub. The panel of the UBE2S WT from Fig 3C is shown for comparison.

B Fluorescent scans monitoring UBE2R2~*Ub in lysine discharge assays. UBE2R2 WT panel from Fig 3D is shown for comparison.

C Equilibrium data fitting of Ub titrations in BLI experiments to detect interactions between Ub and immobilized UBE2R2 variants. Mean data points of $n \geq 3$ independent, technical replicates are shown. Error bars: SD.

D Corresponding raw BLI traces used for equilibrium data fitting in (C).

E Fitting of the METRIS roll parameter data from BLI data.

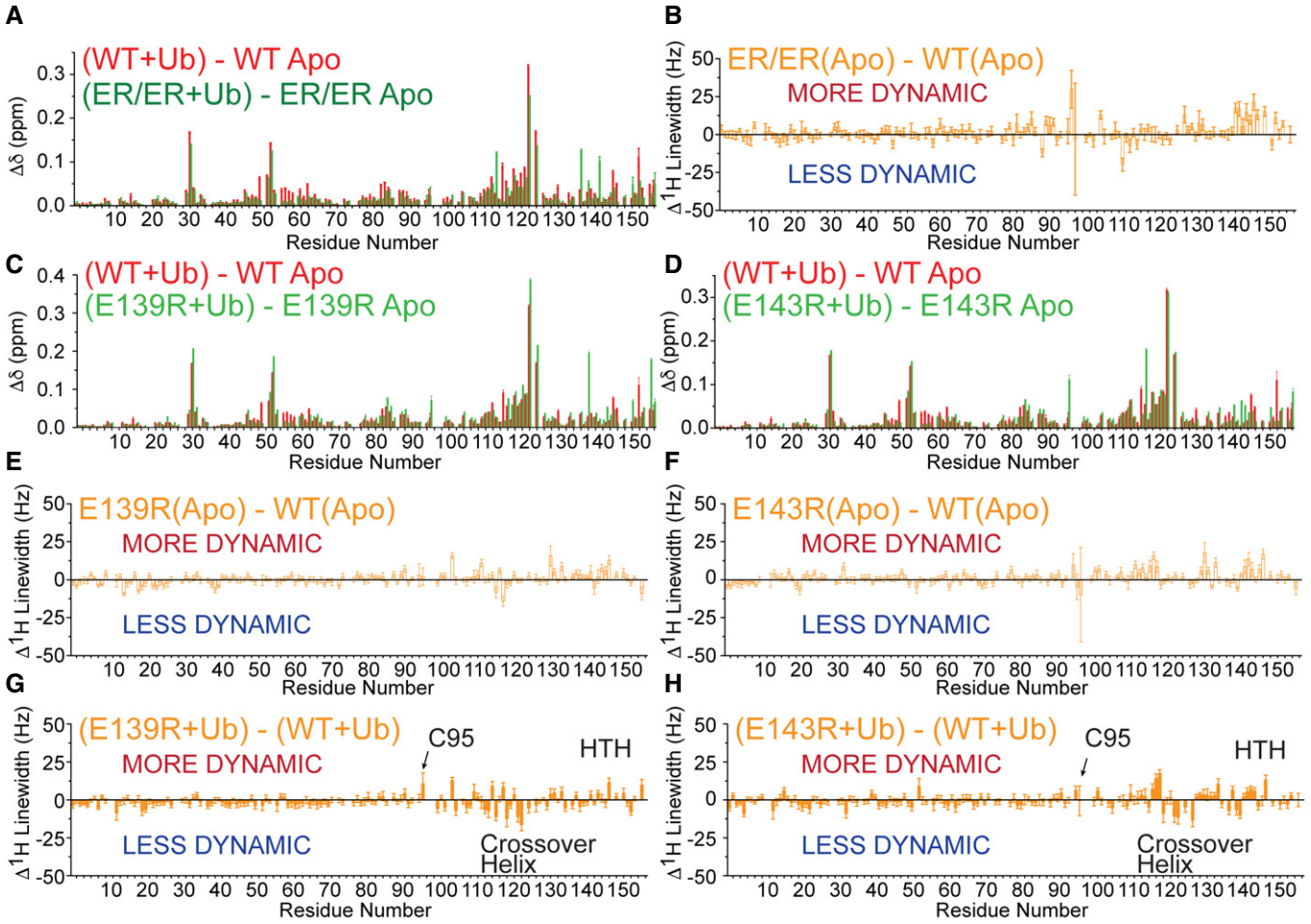

Figure EV4. NMR analysis of UBE2S and its variants binding to Ub.

A NMR chemical-shift perturbations due to the binding of Ub to either UBE2S WT or the ER/ER variant.
B NMR ^{1}H linewidth comparisons of apo (no Ub) UBE2S WT and ER/ER variant.
C, D NMR chemical-shift perturbations due to the binding of Ub to either UBE2S WT or the E139R variant (C) or E143R variant (D).
E, F NMR ^{1}H linewidth comparisons of apo UBE2S WT and E139R (E) or E143R variant (F).
G, H NMR ^{1}H linewidth comparisons of UBE2S WT and E139R (G) or E143R (H) variant when Ub is added.

Data information: (A–H) Shown are the best-fit values and standard deviations (SD) estimated from the covariance matrix analysis of NMR spectra with $n = 2048$ measurement points for 16 ppm in the ^{1}H dimension.

Figure EV5. APC2 competes with the donor Ub to bind to the UBE2S^{HTH}.

A Structure of UBE2C bound to the APC11 RING and APC2 WHB (PDB: 5L9U; Brown *et al*, 2016), demonstrating that the UBE2C^{HTH} is not interacting with the APC/C.
B Representative fluorescent scan (left) and its quantification (right) monitoring CycB* ubiquitination by APC/C and either UBE2C WT or K157E. Data were statistically analyzed using an unpaired Welch's *t*-test (*$P \leq 0.05$, $n = 4$ independent, technical replicates). Error bars: SEM. Data normalized to the unmodified substrate band from reactions lacking an E2.
C Quantification of Fig 6E monitoring the polyubiquitination of Ub-CycB* by a panel of UBE2S^{HTH} charge-swap variants. Data were statistically analyzed by one-way ANOVA (*$P \leq 0.05$, ****$P \leq 0.0001$, $n = 3$ independent, technical replicates). Error bars: SEM. Data normalized to the unmodified substrate band from reactions lacking an E2.
D, E Fluorescent scan (D) and its quantification (E) monitoring APC/C-dependent Ub-Securin (Ub-Sec*) ubiquitination utilizing the panel of UBE2S variants (related to Fig 6E). Data were statistically analyzed by one-way ANOVA ($n = 3$ independent, technical replicates). Error bars: SEM. Data normalized to the unmodified substrate band from reactions lacking an E2.

Source data are available online for this figure.

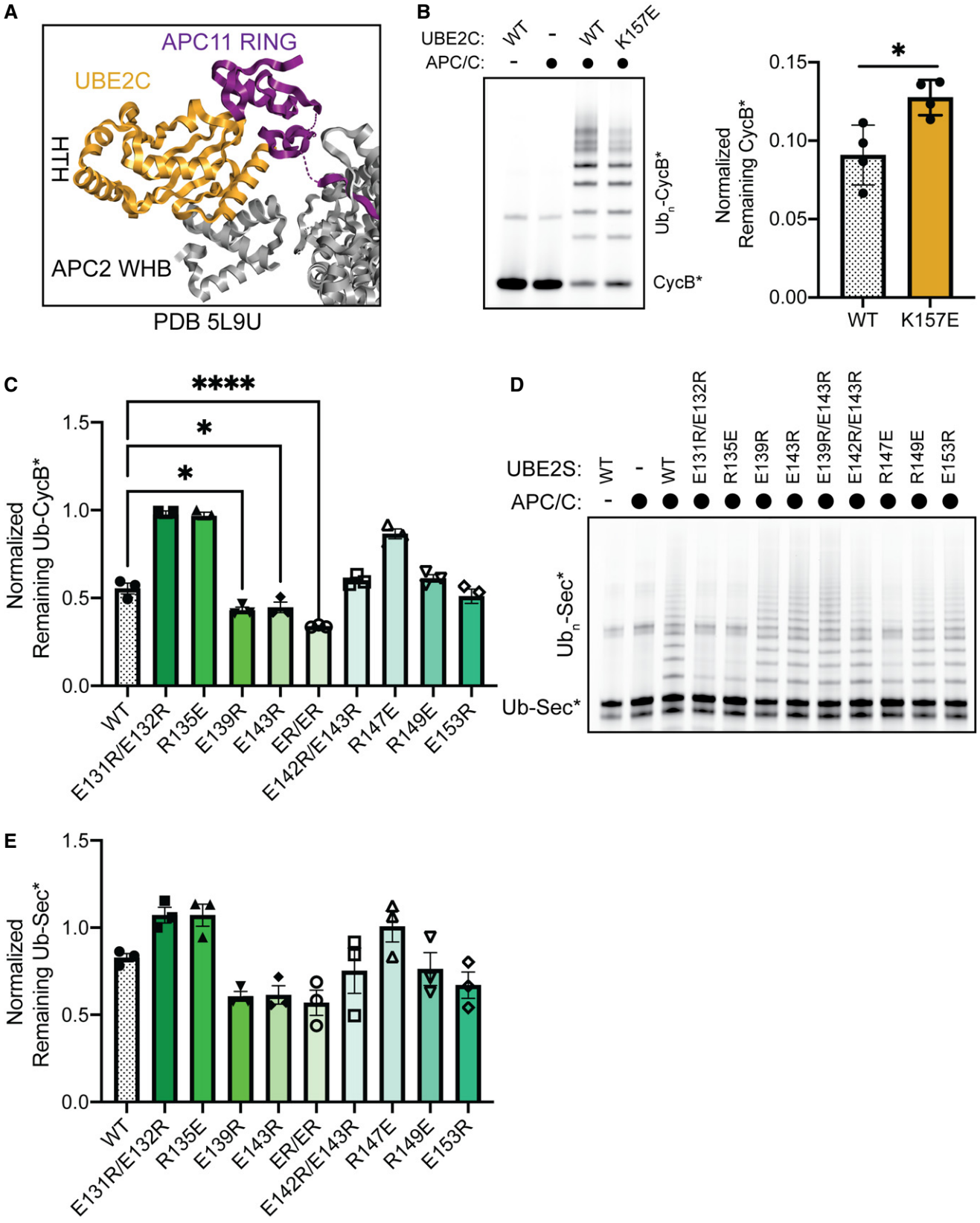

Figure EV5.